

## Lattice Boltzmann model for traffic flow

Jianping Meng,<sup>1,2,\*</sup> Yuehong Qian,<sup>1,†</sup> Xingli Li,<sup>1</sup> and Shiqiang Dai<sup>1</sup>

<sup>1</sup>*Shanghai Institute of Applied Mathematics and Mechanics, Shanghai University, Shanghai 200072, China*

<sup>2</sup>*College of Mathematics, Physics and Information Engineering, Zhejiang Normal University, Jinhua 321004, China*

(Received 15 July 2007; revised manuscript received 12 November 2007; published 6 March 2008)

Mesoscopic models for traffic flows are usually difficult to be employed because of the appearance of integro-differential terms in the models. In this work, a lattice Boltzmann model for traffic flow is introduced on the basis of the existing kinetics models by using the Bhatnagar-Gross-Krook-type approximation interaction term in the Boltzmann equation and discretizing it in time and phase space. The so-obtained model is simple while the relevant parameters are physically meaningful. Together with its discrete feature, the model can be easily used to investigate numerically the behavior of traffic flows. In consequence, the macroscopic dynamics of the model is derived using the Taylor and Chapman-Enskog expansions. For validating the model, numerical simulations are conducted under the periodic boundary conditions. It is found that the model could reasonably reproduce the fundamental diagram. Moreover, certain interesting physical phenomena can be captured by the model, such as the metastability and stop-and-go phenomena.

DOI: [10.1103/PhysRevE.77.036108](https://doi.org/10.1103/PhysRevE.77.036108)

PACS number(s): 89.40.Bb, 47.11.-j, 45.70.Vn, 05.20.Dd

### I. INTRODUCTION

In recent years, traffic modeling has become one of the most exciting fields and attracted many physicists (see [1–4], and references therein). This increasing interest is stimulated not only by its practical implications for optimizing freeway traffic, but also by the observed nonequilibrium phase transitions and various nonlinear dynamical phenomena, such as the formation of traffic jams [5].

Generally speaking, we can classify the traffic models into macroscopic, microscopic, and mesoscopic (especially kinetic) kinds according to the physical ideas. Microscopic models were mainly originated from cellular automata and molecular dynamics (see [1,2,6–8], and references therein). Such models can describe the individual drivers' behavior and their interactions at a high level of details. For instance, the lane-changing behavior is usually described as a detailed chain of drivers' decisions. Evidently microscopic models are mostly used for detailed studies. The most severe drawback of microscopic models is that they will consume an enormous amount of CPU time in simulation if the car number is large. For car-following models, it is because we need to solve a large number of difference equations, and for cellular automaton models, it is needed to repeat the simulation many times in order to improve the signal-to-noise ratio and obtain the statistically meaningful results.

High computational efficiency can be reached by using macroscopic traffic models. Macroscopic traffic models were constructed based on the heuristic analogies with the hydrodynamic equations (see [1–3,9]). They consist of equations for a few aggregate quantities, such as the spatial density  $\rho$ , the average velocity  $V$ , and additional velocity moments. The computational requirement for the macroscopic models mainly depends on the numerical scheme, not on the number of vehicles. Therefore, higher computational efficiency can

be obtained. Due to their heuristic origin, even for the most advanced macroscopic models, there exist some shortcomings [3]. One of the most well-known arguments is the isotropic problem [10] of some previous models [11].

Mesoscopic models belong to the class of stochastic ones which follow the ideas of the gas kinetics theory (see [1–3,12], and references therein). They are mainly based on Boltzmann- or Enskog-type equations for the single vehicle state probability function. From this function, one can calculate the macroscopic flow quantities through averaging and obtain the evolutionary rules governing these quantities. Based on the statistics of the microscopic interactions mechanism, mesoscopic models have almost the same rigorous foundations as the microscopic models, and their parameters are physically meaningful. In principle, the computational efficiency of kinetics models should be between the macroscopic and microscopic models. But, because of its integro-differential feature, mesoscopic models are difficult to be simulated numerically via direct discretization methods. Thus, due to their rigorous foundations, mesoscopic models are often used to derive reasonable macroscopic flow equations via moment or the Chapman-Enskog method in the literature [13,43], e.g., Refs. [5,14,15]. There are only a few papers concerning the direct simulation of the model equations, such as the modified direct simulation Monte Carlo method presented in Ref. [16].

On the other hand, the lattice Boltzmann equation (LBE) method [17–19], which is an innovative computational fluid dynamics method based on the kinetic theory, has attracted significant attention recently in the hydrodynamic research community, especially in the area of complex flows. Historically, the LBE models evolved from their Boolean counterparts, the lattice-gas automata (LGA) [20,21]. The theoretical framework of the LBE has been rested on the Chapman-Enskog analysis of the LGA models though various approximations have been applied, such as the Bhatnagar-Gross-Krook (BGK) approximation [22]. Until very recently the formal connection between the lattice Boltzmann equation and the continuous Boltzmann equation were established [23,24]. It was shown that the lattice Boltzmann equation

\*jpmeng@gmail.com

†Corresponding author. qian@shu.edu.cn

could be considered as a special discretized form of the Boltzmann equation.

In this work, we intend to construct a lattice Boltzmann model for traffic flow, which could also be considered as a discrete version of the continuous kinetic models in analogy to that in the hydrodynamic research. The rest of the paper is organized as follows. In Sec. II, we present the basic idea of the lattice Boltzmann model for traffic flow. The numerical simulations under the periodic conditions are performed to validate the model in Sec. III and Sec. IV is devoted to conclusion and remarks.

## II. MODEL DESCRIPTION

### A. Brief review of continuous kinetic traffic models

For outlining the basic idea of our model, we first give a brief introduction to the framework of the kinetics models for traffic flow. From a mesoscopic point of view, it is usually assumed that the state of an individual vehicle  $\alpha$  at given time  $t$  can be mathematically represented by points in the phase space  $\Omega$ , where the coordinates are the vehicle position  $x_\alpha(t)$ , the vehicle velocity  $v_\alpha(t)$ , and also other quantities characterizing the type or driving style of the vehicles [25]. Thus we can define phase-space density (the velocity distribution of the vehicles) in analogy to the local one-particle reduced distribution function in gas kinetics,

$$f(x, v, t) \Delta x \Delta v = \frac{1}{\Delta t} \int_{t-\Delta t/2}^{t+\Delta t/2} dt' \Delta n(x, v, t'),$$

where  $\Delta n(x, v, t')$  denotes the average number of vehicles that are at a place between  $x - \Delta x/2$  and  $x + \Delta x/2$ , driving with a velocity between  $v - \Delta v/2$  and  $v + \Delta v/2$  at a time  $t' \in [t - \Delta t/2, t + \Delta t/2]$ . Then we can use the phase-space density  $f$  to describe the dynamics of traffic flow, and note that because we only use the ‘‘one vehicle distribution function,’’ all the effects due to the correlations between the vehicles are neglected (i.e., the vehicular chaos assumption). By the definition of the phase-space density, we have the following relations:

$$\rho(x, t) = \int dv f(x, v, t)$$

and

$$q(x, t) = \rho(x, t) V(x, t) = \int dv v f(x, v, t).$$

These relations could be used to obtain the corresponding macroscopic (average) quantities, i.e., the density  $\rho(x, t)$ , the velocity  $V(x, t)$ , or the flow  $q(x, t)$ .

To obtain the equation governing the temporal evolution of the phase-space density  $f$ , we first bring in the well-known fact that the phase-space density obeys the following continuity equation:

$$\frac{\partial f}{\partial t} + \frac{\partial}{\partial x} \left( f \frac{dx}{dt} \right) + \frac{\partial}{\partial v} \left( f \frac{dv}{dt} \right) = \left( \frac{\partial f}{\partial t} \right)_{\text{tr}},$$

where the term  $(\partial f / \partial t)_{\text{tr}}$  delineates the variation of  $f(x, v, t)$  due to discontinuous transitions between various states. All the governing equations in the kinetics models for traffic flow can be mathematically represented by this equation. Prigogine and Herman proposed the first kinetics model for traffic flow [12]. They suggested that the transition term should consist of a relaxation term  $(\partial f / \partial t)_{\text{rel}}$  and an interaction term  $(\partial f / \partial t)_{\text{int}}$  in their model. So the model equation can be written as

$$\frac{\partial f}{\partial t} + \frac{\partial(fv)}{\partial x} + \frac{\partial}{\partial v} \left( f \frac{dv}{dt} \right) = \left( \frac{\partial f}{\partial t} \right)_{\text{rel}} + \left( \frac{\partial f}{\partial t} \right)_{\text{int}}.$$

The relaxation term is intended to describe the drivers' effort (acceleration process) toward their desired speed, and the interaction term to describe the deceleration of vehicles to the velocity of the front car in case that it moves slower and cannot be overtaken.

Let us first consider the relaxation term. Instead of an individual speed adjustment, Prigogine *et al.* suggested a collective relaxation of the actual velocity distribution toward a ‘‘desired’’ velocity distribution  $f_0(x, v, t)$ , which is a mathematical idealization of the goals that the driver population strives to realize [12]. So the term  $\frac{\partial}{\partial v} \left( f \frac{dv}{dt} \right)$  can be ignored in the model and the relaxation term has the form

$$\left( \frac{\partial f}{\partial t} \right)_{\text{rel}} = - \frac{f(x, v, t) - f_0(x, v, t)}{\tau},$$

where  $\tau$  denotes the relaxation time.

For describing the interaction process, Prigogine *et al.* suggested the following Boltzmann-type equation:

$$\begin{aligned} \left( \frac{\partial f}{\partial t} \right)_{\text{int}} &= f(x, v, t) \int_v^\infty d\omega (1-p)(\omega-v)f(x, \omega, t) \\ &\quad - f(x, v, t) \int_0^v d\omega (1-p)(v-\omega)f(x, \omega, t), \end{aligned} \quad (1)$$

i.e.,

$$\left( \frac{\partial f}{\partial t} \right)_{\text{int}} = (1-p)f(x, v, t) \int_0^\infty d\omega (\omega-v)f(x, \omega, t),$$

where  $p$  denotes the probability that a slower car can be overtaken. On the right-hand side of Eq. (1), the first term corresponds to a situation where a vehicle with speed  $\omega > v$  must decelerate to the speed  $v$ , causing an increase of phase-space density, while the second term describes a decrease of phase-space density due to the situation in which vehicles with the velocity  $v$  must decelerate to a velocity  $\omega < v$ . In Ref. [12], one can find a more detailed discussion about the interaction term.

Finally, the Prigogine-Herman model becomes

$$\frac{\partial f}{\partial t} + v \frac{\partial f}{\partial x} = - \frac{f - f_0}{\tau} + (1-p)\rho(V-v)f. \quad (2)$$

Following the pioneering work of Prigogine *et al.*, some authors, e.g., Helbing *et al.* [5,14,26] and Hoogendoorn *et al.* [27,28] have renewed the interest for gas-kinetic models recently. Hoogendoorn *et al.* [28] constructed the generic gas-kinetic traffic model which can be used to describe almost all kinds of traffic situations, even the pedestrian flow. Helbing *et al.* mainly concentrated on the derivation of the continuum traffic models and have developed a program package MASTER based on their model [5,14,26]. Besides the above-mentioned works, there have been many other important works recently which we do not describe in detail here (see Refs. [15,29–36], and references therein).

The drawbacks of the kinetics models are somewhat evident. Despite their assumptions, such as the vehicular chaos assumption, there are a relatively large number of unknown parameters and model relations (e.g., the desired velocity distribution function  $f_0$  and it may be difficult to determine whether the “desired” velocity is just the desired velocity in the realistic observation) that need to be estimated from the observation. Furthermore, their integro-differential-type model equations are usually difficult to be solved with either numerical methods or analytical methods.

### B. Derivation of the lattice Boltzmann model

In this work, the authors try to simplify the kinetic model by introducing the BGK-type interaction term and by discretizing the resultant equation in time and phase space, just as what has been done in hydrodynamics. With the model, it is easy and fast to simulate traffic flow numerically. Furthermore, the parameters and model relation of the model are physically meaningful. First, we consider it reasonable to simplify the interaction term and the individual or collective relaxation term in the kinetics models [e.g., the right-hand side of Eq. (2)] by using a uniform relaxation term toward the local equilibrium velocity distribution [3]. Thus, the BGK-type equation becomes

$$\frac{\partial f}{\partial t} + v \frac{\partial f}{\partial x} = -\frac{f - g_{\text{eq}}}{\lambda}, \quad (3)$$

where  $g_{\text{eq}}$  is the local equilibrium velocity distribution function. In this context, we use the function  $g_{\text{eq}}$  to describe the local equilibrium state resulting from the competition between the two opposite sides in a local region, i.e., the drivers’ effort toward their desired velocity and the interaction with other drivers. Naturally,  $\lambda$  is the relaxation time. Meanwhile,  $g_{\text{eq}}$  obeys the following conservation relation:

$$\rho(x, t) = \int dv f(x, v, t) = \int dv g_{\text{eq}}(x, v, t).$$

Here, the conservation law of momentum or energy does not exist. We can also gain further understanding about  $g_{\text{eq}}$  by multiplying Eq. (3) with  $v^0=1$  and  $v^1$  and integrating with respect to  $v$ . With the above procedure, we could derive the following equations:

$$\frac{\partial \rho}{\partial t} + \frac{\partial(\rho V)}{\partial x} = 0,$$

$$\frac{\partial V}{\partial t} + V \frac{\partial V}{\partial x} = -\frac{1}{\rho} \frac{\partial \mathcal{P}}{\partial x} + \frac{1}{\lambda}(V_{\text{eq}} - V),$$

where

$$V_{\text{eq}}[\rho(x, t)] = \int dv v \frac{g_{\text{eq}}(x, v, t)}{\rho(x, t)},$$

$$\langle v^2 \rangle = \frac{1}{\rho(x, t)} \int dv v^2 f(x, v, t),$$

$$\mathcal{P}(x, t) = \rho(x, t) \{ \langle v^2 \rangle - [V(x, t)]^2 \}.$$

Obviously,  $g_{\text{eq}}$  is the mesoscopic representation of the equilibrium velocity-density relation, i.e., the fundamental diagram.  $\mathcal{P}$  could be considered as the traffic pressure.

Next, we could obtain a formal discretized form of Eq. (3) by use of the technique presented in Refs. [23,24].

First, we formally integrate Eq. (3) over a small time interval  $\delta_t$ ,

$$\begin{aligned} & f(x + v \delta_t, v, t + \delta_t) \\ &= e^{-\delta_t/\lambda} f(x, v, t) + \frac{1}{\lambda} e^{-\delta_t/\lambda} \int_0^{\delta_t} e^{t'/\lambda} g_{\text{eq}}(x + vt', v, t + t') dt'. \end{aligned} \quad (4)$$

Using the Taylor expansion of the right-hand side and neglecting the term of  $O(\delta_t^2)$ , Eq. (4) yields

$$f(x + v \delta_t, v, t + \delta_t) - f(x, v, t) = -\frac{1}{\tau} [f(x, v, t) - g_{\text{eq}}(x, v, t)],$$

where  $\tau \equiv \lambda / \delta_t$  becomes a dimensionless relaxation time. Thus, we have completed the discretization of the time coordinate. The following task is the discretization in the phase space, i.e., in the coordinates  $x$  and  $v$ . According to realistic situations and also for the convenience of comparison with the existing theoretical results, we suggest using a discretization technique similar to the cellular automaton model [6] herein. Namely, a single-lane road can be divided into a one-dimensional array of  $L$  sites and the length of one site is usually set to be 7.5 m. For the velocity coordinate, we let each vehicle move with an integer velocity  $v_i \in \{0, \dots, v_{\text{max}}\}$ , and  $v_{\text{max}}$  is usually set to be 5. Finally, by using the above discretization procedure, we can give the governing equation of the so-called lattice Boltzmann model for traffic flow as follows:

$$f_i(x + v_i \delta_t, t + \delta_t) - f_i(x, t) = \omega [f_i^{\text{eq}}(x, t) - f_i(x, t)], \quad (5)$$

where  $f_i(x, t)$  denotes the distribution of the vehicles moving with velocity  $v_i$ .  $f_i^{\text{eq}}$  denotes the distribution of the vehicles moving with velocity  $v_i$  when the traffic flow is under the local equilibrium state. Obviously,  $f_i^{\text{eq}}$  is the discretization version of  $g_{\text{eq}}$ , i.e., the discretized mesoscopic representation of the equilibrium velocity-density relation.  $\omega$  is the dimensionless relaxation factor, i.e.,  $\omega = 1/\tau$ . In hydrodynamics, one can calculate the appropriate equilibrium distribution function  $f_i^{\text{eq}}$  according to the discretization method of the phase space. But we can only write it as an undetermined

function herein because there is no ‘‘Maxwellian distribution function’’ and a lack of enough conservation laws. We can only determine  $f_i^{\text{eq}}$  through the empirical observation or making assumptions, just as what has been done on the velocity-density relation in the Lighthill-Whitham-Richards (LWR) macroscopic model [9] for obtaining the closed mathematical formulation.

### C. Macroscopic dynamics of the model

In order to validate the discretization method of the phase space and investigate the macroscopic dynamics of the model in more detail, we need to apply the Taylor and Chapman-Enskog expansions for solving Eq. (5). In the derivation, we use the following space scale and two different time scales:

$$t_1 = \epsilon t, \quad t_2 = \epsilon^2 t,$$

$$x_1 = \epsilon x.$$

All of the variables have their respective physical meaning. The small parameter  $\epsilon$ , which plays the role of the Knudsen number, could be considered as the mean vehicle gap over the length of the road. The time scale  $t_1$  is of the order of the time needed to approach the local equilibrium, while the time scale  $t_2$  and space scale  $x_1$  are the scales in which the macroscopic phenomena could be observed.

We first investigate the macroscopic dynamics at the first-order accuracy level. Using the Taylor expansion on the left-hand side of Eq. (5) and neglecting the terms higher than the first order [37], we could obtain

$$\frac{\partial f_i}{\partial t} + v_i \frac{\partial f_i}{\partial x} = \omega(f_i^{\text{eq}} - f_i).$$

Then substituting the above equation with the following asymptotic series

$$f_i = f_i^{\text{eq}} + \epsilon f_i^{(1)} + \epsilon^2 f_i^{(2)} + \dots, \quad (6)$$

we get a series of equations in different orders,

$$\frac{\partial f_i^{\text{eq}}}{\partial t_1} + v_i \frac{\partial f_i^{\text{eq}}}{\partial x_1} + \omega f_i^{(1)} = 0,$$

$$\frac{\partial f_i^{\text{eq}}}{\partial t_2} + \frac{\partial f_i^{(1)}}{\partial t_1} + v_i \frac{\partial f_i^{(1)}}{\partial x_1} + \omega f_i^{(2)} = 0,$$

$$\frac{\partial f_i^{(1)}}{\partial t_2} + \frac{\partial f_i^{(2)}}{\partial t_1} + v_i \frac{\partial f_i^{(2)}}{\partial x_1} + \omega f_i^{(3)} = 0, \quad \dots,$$

$$\frac{\partial f_i^{(N-1)}}{\partial t_2} + \frac{\partial f_i^{(N)}}{\partial t_1} + v_i \frac{\partial f_i^{(N)}}{\partial x_1} + \omega f_i^{(N+1)} = 0.$$

Considering the following relations:

$$\rho(x, t) = \sum_i f_i = \sum_i f_i^{\text{eq}}, \quad (7)$$

$$q(x, t) = \rho(x, t)V(x, t) = \sum_i f_i v_i = \sum_i f_i^{\text{eq}} v_i + \sum_i v_i \sum_{j=1}^N \epsilon^j f_i^{(j)}, \quad (8)$$

$$V_{\text{eq}}[\rho(x, t)] = \sum_i v_i(x, t) \frac{f_i^{\text{eq}}(x, t)}{\rho(x, t)}, \quad (9)$$

and taking the summation in the above equations with respect to  $v$ , we could obtain the following equations:

$$\frac{\partial \rho}{\partial t} + \frac{\partial(\rho V)}{\partial x} = 0,$$

$$\frac{\partial V}{\partial t} + V \frac{\partial V}{\partial x} = -\frac{1}{\rho} \frac{\partial \mathcal{P}}{\partial x} + \omega(V_{\text{eq}} - V). \quad (10)$$

Obviously, at the first-order accuracy level, the macroscopic dynamics of the present model could be recovered as the macroscopic equations we have derived before in Sec. II B (one can also refer to Eqs. (40) and (41) in Ref. [14]). Thus, the discretization method of the phase space is also proved to be reasonable.

Next, we try to investigate the macroscopic dynamics further at the second-order accuracy level, i.e., to solve the following equation:

$$\frac{\partial f_i}{\partial t} + v_i \frac{\partial f_i}{\partial x} + \frac{v_i^2}{2} \left( \frac{\partial^2 f_i}{\partial x^2} \right) + v_i \left( \frac{\partial^2 f_i}{\partial x \partial t} \right) + \frac{1}{2} \left( \frac{\partial^2 f_i}{\partial t^2} \right) = \omega(f_i^{\text{eq}} - f_i). \quad (11)$$

Using the above procedure again, we first substitute Eq. (6) into Eq. (11) and obtain the equation in the  $\epsilon^0$ ,  $\epsilon^1$ , and  $\epsilon^2$  orders,

$$\epsilon^0, \quad 0 = 0;$$

$$\epsilon^1, \quad \frac{\partial f_i^{\text{eq}}}{\partial t_1} + v_i \frac{\partial f_i^{\text{eq}}}{\partial x_1} + \omega f_i^{(1)} = 0;$$

$$\epsilon^2, \quad \frac{\partial f_i^{\text{eq}}}{\partial t_2} + \frac{\partial f_i^{(1)}}{\partial t_1} + v_i \frac{\partial f_i^{(1)}}{\partial x_1} + \omega f_i^{(2)} + \frac{1}{2} \left( \frac{\partial^2 f_i^{\text{eq}}}{\partial t_1^2} \right) + v_i \left( \frac{\partial^2 f_i^{\text{eq}}}{\partial x_1 \partial t_1} \right) + \frac{v_i^2}{2} \left( \frac{\partial^2 f_i^{\text{eq}}}{\partial x_1^2} \right) = 0.$$

Considering the relations (7)–(9) and the additional fact that

$$\begin{aligned} & \frac{1}{2} \left( \frac{\partial^2 f_i^{\text{eq}}}{\partial t_1^2} \right) + v_i \left( \frac{\partial^2 f_i^{\text{eq}}}{\partial x_1 \partial t_1} \right) + \frac{v_i^2}{2} \left( \frac{\partial^2 f_i^{\text{eq}}}{\partial x_1^2} \right) \\ &= \frac{1}{2} \frac{\partial}{\partial t_1} \left( \frac{\partial f_i^{\text{eq}}}{\partial t_1} + v_i \frac{\partial f_i^{\text{eq}}}{\partial x_1} \right) + \frac{v_i}{2} \frac{\partial}{\partial x_1} \left( \frac{\partial f_i^{\text{eq}}}{\partial t_1} + v_i \frac{\partial f_i^{\text{eq}}}{\partial x_1} \right) \\ &= -\frac{\omega}{2} \left( \frac{\partial f_i^{(1)}}{\partial t_1} + v_i \frac{\partial f_i^{(1)}}{\partial x_1} \right), \end{aligned}$$

$$\mathcal{P}_{\text{eq}} = \sum_i v_i^2 f_i^{\text{eq}} - \rho(x, t)V_{\text{eq}}^2,$$

we could derive the following equations by taking the summation with respect to  $v$ :

$$\begin{aligned} \frac{\partial \rho}{\partial t_1} + \frac{\partial(\rho V_{\text{eq}})}{\partial x_1} &= 0, \\ \frac{\partial \rho}{\partial t_2} &= \left( \frac{1}{\omega} - \frac{1}{2} \right) \frac{\partial}{\partial x_1} \left( \frac{\partial \sum_i v_i f_i^{\text{eq}}}{\partial t_1} + \frac{\partial \sum_i v_i^2 f_i^{\text{eq}}}{\partial x_1} \right) \\ &= \left( \frac{1}{\omega} - \frac{1}{2} \right) \frac{\partial}{\partial x_1} \left[ \left( V_{\text{eq}} + \rho \frac{\partial V_{\text{eq}}}{\partial \rho} \right) \frac{\partial \rho}{\partial t_1} + \frac{\partial \mathcal{P}_{\text{eq}}}{\partial x_1} + \frac{\partial(\rho V_{\text{eq}}^2)}{\partial x_1} \right] \\ &= \left( \frac{1}{\omega} - \frac{1}{2} \right) \frac{\partial}{\partial x_1} \left[ \frac{\partial \mathcal{P}_{\text{eq}}}{\partial x_1} + \frac{\partial(\rho V_{\text{eq}}^2)}{\partial x_1} \right. \\ &\quad \left. - \left( V_{\text{eq}} + \rho \frac{\partial V_{\text{eq}}}{\partial \rho} \right) \frac{\partial(\rho V_{\text{eq}})}{\partial x_1} \right]. \end{aligned}$$

Finally we could obtain the equation with the normal space and time scale,

$$\begin{aligned} \frac{\partial \rho}{\partial t} + \frac{\partial(\rho V_{\text{eq}})}{\partial x} &= \left( \frac{1}{\omega} - \frac{1}{2} \right) \frac{\partial}{\partial x} \left[ \frac{\partial \mathcal{P}_{\text{eq}}}{\partial x} + \frac{\partial(\rho V_{\text{eq}}^2)}{\partial x} \right. \\ &\quad \left. - \left( V_{\text{eq}} + \rho \frac{\partial V_{\text{eq}}}{\partial \rho} \right) \frac{\partial(\rho V_{\text{eq}})}{\partial x} \right]. \end{aligned} \quad (12)$$

It is a density evolutionary equation and can be considered a so-called scalar model [3] [cf. Eq. (4) in Ref. [14] and Eqs. (5.7) and (5.12) in Ref. [3]]. Though it is quite complex, we could still find the diffusionlike term in the equation. However, it is difficult to derive directly the velocity evolutionary equation at the second-order accuracy level due to the lack of the conservation law of momentum.

In the following, the stability of the solutions to Eq. (12) will be investigated based on the linear stability analysis since the stability is concerned with some important realistic phenomena, e.g., the stop-and-go traffic. We know that the homogeneous solution of Eq. (12) is  $\rho(x, t) = \rho_e$  and  $V(x, t) = V_{\text{eq}}(\rho_e)$ .  $\rho_e$  denotes the average vehicle density on the entire road. Then, we suppose a small perturbation  $\sigma(x, t)$  and the equation for  $\sigma$  can be obtained by substituting the relation (13) into Eq. (12),

$$\rho(x, t) = \rho_e + \sigma(x, t). \quad (13)$$

In the substitution, the following relations must be used:

$$\theta(\rho) = \frac{dV_{\text{eq}}(\rho)}{d\rho}, \quad \phi(\rho) = \frac{d\mathcal{P}_{\text{eq}}(\rho)}{d\rho},$$

$$V_{\text{eq}}(\rho_e + \sigma) = V_{\text{eq}}(\rho_e) + \theta(\rho_e)\sigma,$$

$$\theta(\rho_e + \sigma) = \theta(\rho_e) + \theta'(\rho_e)\sigma,$$

$$\mathcal{P}_{\text{eq}}(\rho_e + \sigma) = \mathcal{P}_{\text{eq}}(\rho_e) + \phi(\rho_e)\sigma,$$

where the Taylor expansion is used for  $V_{\text{eq}}$ ,  $\mathcal{P}_{\text{eq}}$ , and  $\theta$  and terms above the first order are omitted. After some algebra, one obtains the following linearized equation:

$$\begin{aligned} \frac{\partial \sigma}{\partial t} + [V_{\text{eq}}(\rho_e) + \rho_e \theta(\rho_e)] \frac{\partial \sigma}{\partial x} \\ = \left( \frac{1}{\omega} - \frac{1}{2} \right) [\phi(\rho_e) - \theta^2(\rho_e) \rho_e^2] \frac{\partial^2 \sigma}{\partial x^2}. \end{aligned} \quad (14)$$

The following form of the perturbation wave is supposed and substituted into Eq. (14):

$$\sigma = \tilde{\rho} \exp(ikx - \gamma t),$$

$$\gamma = \mu + iv,$$

where  $k$  must satisfy some certain conditions described in Ref. [38] under the periodic boundary conditions. Finally, the equation for  $\mu$  is obtained,

$$\mu = \frac{k^2(2 - \omega)[\phi(\rho_e) - \theta^2(\rho_e)\rho_e^2]}{2\omega}. \quad (15)$$

From the above equation, the stability of Eq. (12) does not depend on the wave number  $k$ . Moreover, considering the general numerical stability conditions  $0 \leq \omega \leq 2$  [39], the stability only depends on the choice of  $V_{\text{eq}}(\rho)$ , i.e.,  $f_i^{\text{eq}}$ . If the value  $\kappa = \phi(\rho_e) - \theta^2(\rho_e)\rho_e^2$  becomes negative, the homogeneous state loses its stability. Therefore,  $f_i^{\text{eq}}$  must be selected carefully for reproducing the observed rich traffic phenomena.

### III. NUMERICAL SIMULATION FOR VALIDATING THE MODEL

In order to validate further the model, we conduct some numerical simulations. First, we must propose a specific distribution  $f_i^{\text{eq}}$ . Obviously, the most reliable way for this purpose is to construct this distribution from the observation data, and  $f_i^{\text{eq}}$  must have the following additional properties: when  $\rho$  is very small, the equilibrium distribution  $f_{v_{\text{max}}}^{\text{eq}}$  of the vehicles moving with the maximum velocity  $v_{\text{max}}$  should be much larger than that of the other velocities (in an ideal case,  $f_{v_{\text{max}}}^{\text{eq}}$  should be close to  $\rho$ ). In contrast, as  $\rho$  is sufficiently large,  $f_0^{\text{eq}}$  should be much larger than that of the other velocities. Herein, we propose the following distribution function to describe the empirical phenomena:

$$f_{n,i}^{\text{eq}} = \frac{v_i^2 \exp\left(-\frac{v_i^2 \rho'^2}{1 - \rho'}\right) \rho_n}{1 + \sum_{i=1}^5 v_i^2 \exp\left(-\frac{v_i^2 \rho'^2}{1 - \rho'}\right)}, \quad (16)$$

$$f_{n,0}^{\text{eq}} = \frac{\rho_n}{1 + \sum_{i=1}^5 v_i^2 \exp\left(-\frac{v_i^2 \rho'^2}{1 - \rho'}\right)}, \quad (17)$$

$$\rho' = \frac{\sum_{i=0}^5 \rho_{n+i}}{6}, \quad (18)$$

where  $\rho_k$  denotes the density at the  $k$ th sites. In this distribution function, the status of the five ahead sites have been considered to describe the forwardly directed interactions, since the car can move forward at most five sites (the maximum velocity has been set to be five by default); in other words, the most important influence comes from the five ahead sites.

For avoiding the occurrence of the nonphysical density (greater than the maximum density), it is necessary to treat a site as a “virtual boundary” varying with time in the numerical simulation. The fact can be easily understood as that if there is a vehicle at the  $n$ th site at some time, the vehicles behind this site (upstream) cannot go through or into this site. Thus, the behavior of the site is very similar with that of the boundary varying with time in the hydrodynamic research [40]. To explain more clearly, for the  $n$ th site, the sum of the distribution which will transfer into or stay at this site cannot exceed the maximum possible maximum density  $\rho_{\max}$ . If  $\rho_n$  at the destination  $n$ th site for a distribution  $f_i$  of  $v_i \neq 0$  at the  $k$ th site (behind the  $n$ th site) already reaches the maximum density,  $f_i$  should be converted into  $f_{i-1}$  (equivalently as the slowing down process). In addition, since different distributions (five by default) at different upstream sites can transfer into one destination site, the priority is determined according to the distance from the destination site, and the shorter distance means the higher priority. Therefore, the actual interaction-transfer process of the distribution function can be divided into the following three substeps: (1) Distribution updates according to Eqs. (16)–(18); (2) distribution updates due to the “virtual boundary”; (3) transfer of the distribution function [41].

Before conducting the specific simulations, some characteristics of the model with Eqs. (16)–(18) can be discussed by using the result of the above linear stability analysis. Since the homogeneous solution  $\rho_e$  is a constant, one can obtain the fundamental diagrams [see Fig. 1(a)] assumed by Eqs. (16)–(18). The stability region of Eq. (12) is shown in Fig. 1(b). Thus, one can predict that the discrete model equation (5) with Eqs. (16)–(18) may capture some basic interesting traffic phenomena, e.g., stop-and-go traffic. The conclusion will be verified further by the following numerical simulations.

First, we check the ability for reproducing the fundamental diagram. For this purpose, a system of 10 000 sites is considered under the periodic boundary conditions. The length of each site is set to be 7.5 m (i.e., a road of 75 km long is simulated).  $\delta_t$  (the time step) is set to be 1 s and  $v_{\max}$  is set to be 5 sites/time step (i.e., 135 km/h). Vehicles are initially distributed randomly on the sites, after a transient period  $t_0$  ( $t_0=2000$  time steps); we calculate the space-averaged velocity at each time step in the period of  $T$  (1000 time steps) and then make the time average for these velocity values. Thus we obtained the average flow in one run, i.e.,

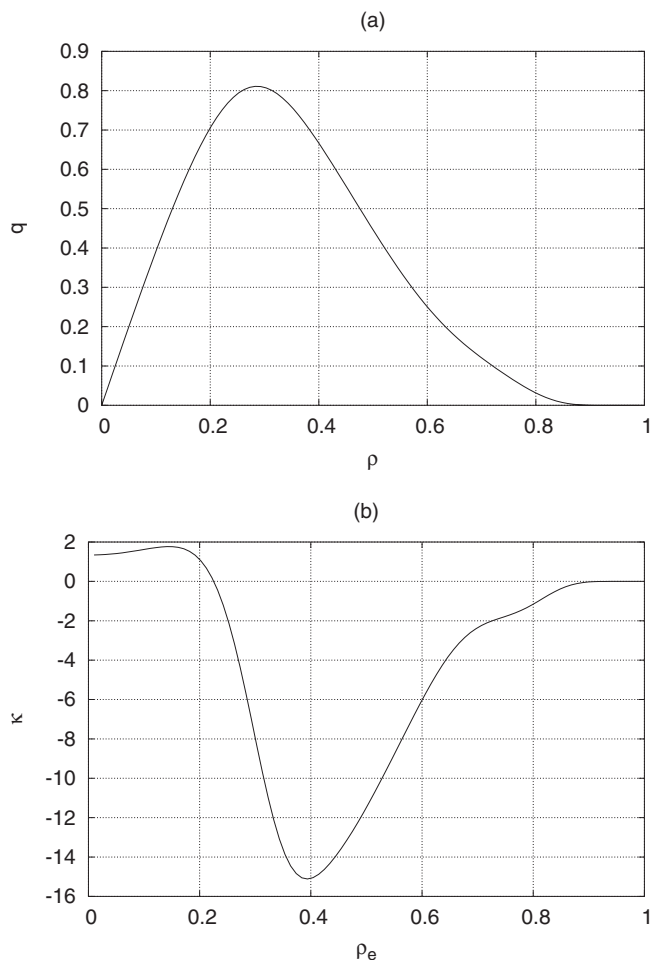


FIG. 1. (a) The fundamental diagram assumed by Eqs. (16)–(18); (b) the stability region given that the road has an infinite length of Eq. (12). Only the value of  $\kappa = \phi(\rho_e) - \theta^2(\rho_e)\rho_e^2$  is depicted.

$$\langle q \rangle = \frac{1}{T} \sum_{t=1}^T \left[ \frac{1}{N} \sum_{n=1}^N \left( \sum_{i=0}^{v_{\max}} v_{n,i} f_{n,i} \right) \right],$$

where  $N$  denotes the total number of sites and  $n$  the position of  $f_i$ .  $\langle q \rangle$  is the average flow. In Fig. 2, each point represents an average value of 10 runs [42].

In Fig. 2, we show the simulation result of the fundamental diagram. For the convenience of comparison, we also present the result obtained with the NaSch model [6] in Fig. 2, and moreover, one can compare the result with the observation (e.g., Fig. 5 in Ref. [6]). The numerical result shows that the present discrete model can reproduce the fundamental diagram with the chosen  $f_i^{\text{eq}}$ . The most basic physical fact, i.e., the phase transition from the free flow to the congested flow, can be explained, especially, the computational speed for obtaining the fundamental diagram is considerably high since the statistical noise is reduced in this discrete kinetics model, i.e., the computational time for the averaging process can be saved. In addition, we notice that the computational resource needed for the simulation based on the present model does not depend on the number of vehicles. Thus,

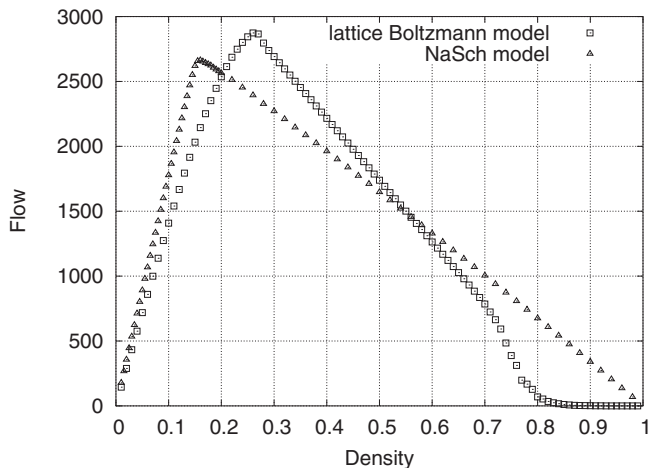


FIG. 2. The simulation result of the fundamental diagram obtained with the present lattice Boltzmann model. For comparison, the result of the NaSch model (with the randomization probability  $P_{dec}=0.05$ ) is also presented.

compared with microscopic models, the model has certain advantages when the number of vehicles is large.

In order to investigate numerically the detailed characteristics of the model, a small perturbation will be introduced at

the initial time. For convenience, the periodic boundary condition is also adopted and for reducing the finite size effect as much as possible, a system of 100 000 sites (750 km) is considered while only the traffic situation on a section will be observed. At the beginning of the simulation, we assume an equilibrium traffic state and a localized density perturbation is added in a certain road section. The simulation results are presented in Fig. 3.

The simulations show that with the present  $f_i^{eq}$ , the model can capture the basic physical phenomena, such as the metastability [Figs. 3(b) and 3(c)] and stop-and-go traffic [Fig. 3(d)]. When the density is small enough the system is stable [Fig. 3(a)]. The results confirm the conclusion of the linear stability analysis of Eq. (12).

IV. DISCUSSION AND CONCLUDING REMARKS

In summary, we have proposed a lattice Boltzmann model for traffic flow. The model could be considered as a discrete version of kinetic models and derived formally from the existing continuous kinetic models. The proposed model has been confirmed to overcome the principal drawback of the latter: the integro-differential nature. In order to validate the discretization method of the phase space and investigate the macroscopic dynamics of the model in more details, we have

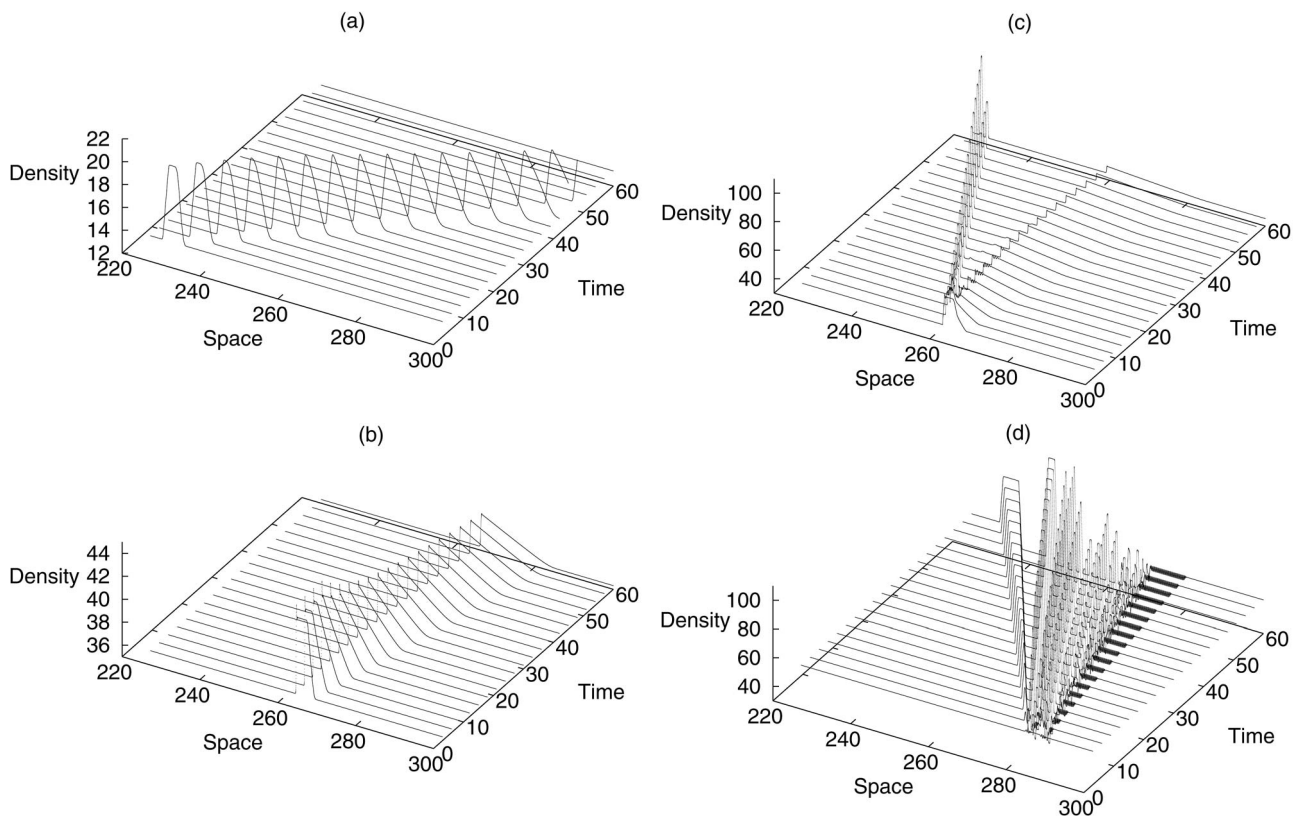


FIG. 3. Spatial-temporal evolution of the traffic density  $\rho(x,t)$ . A system of 100 000 sites (750 km) is modeled and the section 30 000th–40 000th site (75 km) is observed. A 500-site (3.75 km) wide localized perturbation is added. For the convenience of observation, the perturbation will be added in the different road section for the four simulations. The amplitude of the perturbation is (a) 0.05 (6.7 vehicles/km) for free and stable traffic at the initial homogeneous density 0.1 (13.3 vehicles/km); (b) 0.05 for metastable traffic at 0.265 (35.3 vehicles/km); (c) 0.15 (20 vehicles/km) at 0.265; (d) 0.05 for unstable traffic at 0.4 (53.3 vehicles/km). The unit for time in the figures is minutes, and the units for density and space are scaled to vehicles/km and km, respectively.

applied the Taylor expansion and Chapman-Enskog expansion to study the model equation. The first- and second-order macroscopic dynamics are derived and the discretization method of the phase space is shown to be appropriate. In addition, the stability of the derived second-order macroscopic equation is analyzed based on the linear stability theory. The analysis shows that the stability of the model depends mainly on the choice of the local equilibrium velocity distribution function.

By choosing an appropriate local equilibrium velocity distribution function, we have run simulations to verify the capability of the model for simulating traffic flow. It has been found that the model could reproduce the fundamental diagram. The most basic physical fact of the phase transition from the free flow to the congested flow could be explained.

Further simulations show the model could capture the basic physical phenomena, such as the metastability and stop-and-go traffic.

#### ACKNOWLEDGMENTS

This work was partially supported by the National Basic Research Program of China (Grant No. 2006CB705500), the National Natural Science Foundation of China (Grant Nos. 10532060 and 10625210), the Special Research Fund for the Doctoral Program in Higher Education of China (Grant No. SRFDP 20040280014), the Science and Technology Committee of Shanghai (Grant Nos. 05ZR1449 and 07PJ14040), and the Scientific Research Project of the Department of Education of Zhejiang Province (Grant No. 20050306).

- 
- [1] D. Chowdhury, L. Santen, and A. Schadschneider, *Phys. Rep.* **329**, 199 (2000).
- [2] D. Helbing, *Rev. Mod. Phys.* **73**, 1067 (2001).
- [3] N. Bellomo, M. Delitala, and V. Coscia, *Math. Models Meth. Appl. Sci.* **12**, 1801 (2002).
- [4] S. Q. Dai, S. W. Feng, and G. Q. Gu, *Ziran Zazhi* **19**, 196 (1997) (in Chinese).
- [5] M. Treiber, A. Hennecke, and D. Helbing, *Phys. Rev. E* **59**, 239 (1999).
- [6] K. Nagel and M. Schreckenberg, *J. Phys. I* **2**, 2221 (1992).
- [7] L. A. Pipes, *J. Appl. Phys.* **24**, 274 (1953).
- [8] M. Bando, K. Hasebe, A. Nakayama, A. Shibata, and Y. Sugiyama, *Phys. Rev. E* **51**, 1035 (1995).
- [9] M. J. Lighthill and G. B. Whitham, *Proc. R. Soc. London, Ser. A* **229**, 317 (1955); P. I. Richards, *Oper. Res.* **4**, 42 (1956).
- [10] The isotropic problem has been solved by several models, such as the gas-kinetic-based traffic model [5,26]. One can refer to Ref. [2] (p. 1098) for a detailed list.
- [11] C. F. Daganzo, *Transp. Res., Part B: Methodol.* **29**, 277 (1995).
- [12] Ilya Prigogine and Robert C. Herman, *Kinetic Theory of Vehicular Traffic* (Elsevier, New York, 1971).
- [13] Interestingly, Ref. [43] provided another scheme to derive the macroscopic equations from the car-following models. Therein, the derivation process is somewhat different from those based on the kinetics models.
- [14] D. Helbing, *Phys. Rev. E* **53**, 2366 (1996).
- [15] R. M. Velasco and W. Marques, Jr., *Phys. Rev. E* **72**, 046102 (2005).
- [16] K. T. Waldeer, *Comput. Phys. Commun.* **156**, 1 (2003).
- [17] R. Benzi, S. Succi, and M. Vergassola, *Phys. Rep.* **222**, 145 (1992).
- [18] Y. H. Qian, D. d’Humières, and P. Lallemand, *Europhys. Lett.* **17**, 479 (1992).
- [19] H. D. Chen, S. Y. Chen, and W. H. Matthaeus, *Phys. Rev. A* **45**, R5339 (1992).
- [20] U. Frisch, B. Hasslacher, and Y. Pomeau, *Phys. Rev. Lett.* **56**, 1505 (1986).
- [21] S. Wolfram, *J. Stat. Phys.* **45**, 471 (1986).
- [22] P. L. Bhatnagar, E. P. Gross, and M. Krook, *Phys. Rev.* **94**, 511 (1954).
- [23] X. Y. He and L. S. Luo, *Phys. Rev. E* **55**, R6333 (1997).
- [24] X. Y. He and L. S. Luo, *Phys. Rev. E* **56**, 6811 (1997).
- [25] For brevity, we will only consider the position and velocity coordinates in the following context; the other coordinates will be considered only if necessary.
- [26] D. Helbing, A. Hennecke, V. Shvetsov, and M. Treiber, *Transp. Res., Part B: Methodol.* **35**, 183 (2001).
- [27] S. P. Hoogendoorn and P. H. L. Bovy, *Transp. Res., Part B: Methodol.* **34**, 123 (2000).
- [28] S. P. Hoogendoorn and P. H. L. Bovy, *Transp. Res., Part B: Methodol.* **35**, 317 (2001).
- [29] V. Coscia, M. Delitala, and P. Frasca, *Int. J. Non-Linear Mech.* **42**, 411 (2007).
- [30] Marcello Delitala, *C. R. Mec.* **331**, 817 (2003).
- [31] H. J. Cho and S. C. Lo, *Physica A* **312**, 342 (2002).
- [32] A. Sopasakis, *Math. Comput. Modell.* **35**, 623 (2002).
- [33] M. Lo Schiavo, *Math. Comput. Modell.* **35**, 607 (2002).
- [34] P. Nelson and A. Sopasakis, *Transp. Res., Part B: Methodol.* **32**, 589 (1998).
- [35] A. Klar and R. Wegener, *J. Stat. Phys.* **87**, 91 (1997).
- [36] D. Helbing, *Physica A* **242**, 175 (1997).
- [37] For convenience and without losing generality,  $\delta_i$  is supposed to be 1 in the following derivation. It accords with the usual numerical simulation time step 1 s. In fact, one only needs to change the parameter  $\omega$  in Eq. (10) to  $\frac{1}{\lambda}$  and multiply a positive constant  $\delta_i$  on the right-hand side of Eq. (12) if  $\delta_i$  is considered. Thus, the simplification does not influence the following discussion on the stability.
- [38] B. S. Kerner and P. Konhäuser, *Phys. Rev. E* **48**, R2335 (1993).
- [39] *Lattice-Gas Cellular Automata and Lattice Boltzmann Models: An Introduction*, edited by Dieter A. Wolf-Gladrow, *Lect. Notes Math.* Vol. 1725 (Springer, New York, 2000), Chap. 5.
- [40] P. Lallemand and L. S. Luo, *J. Comput. Phys.* **184**, 406 (2003).
- [41] The introduction of “virtual boundary” will induce an artificial perturbation when one implements the numerical simulation under the periodic boundary conditions. Since there is no leading site with the periodic boundary conditions but the “virtual



boundary” mechanism needs one, the artificial effect will be introduced. Nevertheless, one could use the average process and a road long enough to reduce the effect of the artificial perturbation in the following simulations while such an artificial effect does not exist with open boundary conditions.

[42] Herein, a global measurement as used in the cellular automaton model is taken for the convenience of comparison. As it has been shown, the transient period time and the sample number needed in the present model to obtain the fundamental

diagram are less than that of the NaSch model. Thus, the computational time could be reduced. For instance, for the result presented in Fig. 2(a), about 2.5 hours is needed on a Pentium D 2.8 GHz PC, while a typical numerical simulation (10 000 time steps transient period and 30 runs) of the NaSch model for the same size system needs about 10 hours on the same computer.

[43] H. K. Lee, H.-W. Lee, and D. Kim, Phys. Rev. E **64**, 056126 (2001).